Solvation Dynamics of Li^+ and Cl^- Ions in Liquid Methanol

Marco Pagliai,† Gianni Cardini,*,†,‡ and Vincenzo Schettino†,‡

Laboratorio di Spettroscopia Molecolare, Dipartimento di Chimica, Università di Firenze, Via della Lastruccia 3, 50019 Sesto Fiorentino, Firenze, Italy, and European Laboratory for Nonlinear Spectroscopy (LENS), via Nello Carrara 1, 50019 Sesto Fiorentino, Firenze, Italy

Received: January 25, 2005

Car−Parrinello molecular dynamics simulations have been performed on Li^+ and Cl^- in fully deuterated liquid methanol. The results have been compared with available experimental and theoretical data. It has been found that the lithium cation has a stable tetrahedral coordination, whereas the chloride anion presents an average coordination number of 3.56. The polarization effects induced by the ion on the solvent have been analyzed in terms of Wannier function centers. Particular attention has been devoted to the charge transfer, which is particularly important in these types of systems. Evidence for the stability of the lithium cation solvent cage also has been found in the vibrational spectra.

1. Introduction

The solvation dynamics of ions in polar solvents is a topic of current interest in chemical physics, with implications in biochemical, medical, and technological research.[1] Despite the wide range of solvents generally used in practice, for different motivations theoretical studies have mainly been carried out on water and ammonia. In fact, in the case of water the interest is essentially related to the nature of the interactions in the hydration process of the ions in biological environments, like, for example, the selectivity of a protein channel with respect to K^+ rather than to Na^+.[2−5] In the case of ammonia the electron solvation properties have been deeply analyzed, especially in the case of lithium atom.[6,7] Only a limited number of studies have been devoted to other solvents, like methanol,[8−13] methylamine,[8] and acetonitrile.[12,14,15]

In the present work, the solvation of Li^+ and Cl^- in liquid methanol will be analyzed by ab initio molecular dynamics within the Car−Parinello (CPMD)[16−18] formalism. Studies on the interactions between cations[19−30] or anions[21,30−35] and the solvent have been successfully performed with CPMD both in water and in ammonia, showing that the more relevant terms of interaction are limited to the first solvation shell. Open questions are related to the role of the cation or of the anion on the actual stability of the first solvation shell. The interactions between anions and protic solvent has been analyzed and explained in terms of hydrogen bonding, while for the cation−solvent interaction a clear picture is still lacking. In particular, an evaluation of the charge-transfer effects is missing, even though in the past few years there has been a growing interest in the charge transfer between the solvent and a series of systems ranging from simple ions to biological molecules.[33,36−40] In an attempt to rationalize and illustrate the charge reorganization in the environment of the Cl^- and Li^+ ions in methanol, a series of populational analyses based both on the Atoms in Molecules (AIM)[41] and on the Wannier Functions Centers (WFC)[42,43] procedures have been performed. The AIM method is strongly related to the electronic density[41,44,45] and based on the partitioning of this quantity and results to be almost basis set independent.[46] This approach has been successfully adopted in studies of charge transfer in H-bonded molecular clusters.[47,48] Additional information on the polarizability of the solvent can be obtained from the WFCs analysis that allows also the estimate of the induced polarization of the ion[21,49−51] and the dipole moment of molecules in pure liquids.[18,52−57]

2. Computational Details

The simulations have been performed with the CPMD code[16] in a cubic box of 12.05 Å length, with periodic boundary conditions and 25 methanol molecules and one ion. Two systems, one containing Li^+ and the other Cl^-, have been studied, starting from a configuration extracted from a previous Car−Parrinello simulation on fully deuterated liquid methanol.[52]

Martins−Troullier[58] pseudopotentials have been used along with the Kleinman−Bylander[59] decomposition for the C, O, and Cl atomic species, whereas a Goedecker[60] pseudopotential has been adopted for lithium and a von Barth−Car[29] pseudopotential for the hydrogen. The plane wave expansions have been truncated at 70 Ry. Density functional calculations in the generalized gradient approximation (GGA) have been performed by using the BLYP[61,62] exchange correlational functional.

To validate the computatational strategy adopted, the structure and some of the electronic properties of the CH_3OH complex with both Li^+ and Cl^- ions have been calcuated with our approach and compared with DFT and MP2 calculations with a localized Gaussian basis set, 6-311++G(d,p). The results, summarized in Table 1, show that the BLYP functional in conjunction with the plane wave basis set satisfactorily reproduce the structural parameters of both complexes, while the binding energy is close to the other DFT calculations and slighly lower than at the MP2 level of theory, but with the usual error (10 kJ mol^{-1}) of this kind of calculation.

The amount of charge transferred on the ions (Δq) has been computed within the AIM[41] formalism. The Δq values are essentially the same at all levels of theory adopted, with only small differences related to the semicore pseudopotential of the lithium atom (core and valence electrons are taken into account).

The deuterium has been used instead of hydrogen to allow for a larger time-step. A ficticious electronic mass of 800 au

* Address correspondence to this author.
† Università di Firenze.
‡ European Laboratory for Nonlinear Spectroscopy (LENS).

10.1021/jp050428q CCC: $30.25
Published on Web 03/19/2005

TABLE 1: Binding Energy, Charge Transferred on the Ions, and Salient Structural Data of the Complexes $CH_3OH\cdots Li^+$ and $CH_3OH\cdots Cl^-$[a]

	BLYP/PW	BLYP/G	B3LYP/G	MP2/G
$CH_3OH\cdots Li^+$				
$r_{(O\cdots Li)}$	1.814	1.829	1.818	1.845
$r_{(OH)}$	0.975	0.975	0.965	0.964
$r_{(CO)}$	1.499	1.489	1.467	1.459
$r_{(HC)}$	1.091	1.095	1.089	1.089
$\alpha_{(LiOH)}$	123.334	123.481	123.183	123.440
$\alpha_{(LiOC)}$	129.031	128.495	128.296	128.884
$E_{binding}$, kJ mol^{-1}	−164.85	−163.41	−166.43	−155.61
$\Delta q(e^-)$	−0.06	−0.09	−0.09	−0.08
$CH_3OH\cdots Cl^+$				
$r_{(H\cdots Cl)}$	2.093	2.124	2.130	2.084
$r_{(H\cdots O)}$	3.097	3.122	3.109	3.053
$r_{(OH)}$	1.008	1.005	0.991	0.986
$r_{(CO)}$	1.432	1.424	1.407	1.407
$r_{(HC)}$	1.101	1.107	1.099	1.098
$\alpha_{(ClOH)}$	173.645	171.475	169.657	166.883
$E_{binding}$, kJ mol^{-1}	−65.10	−63.81	−64.40	−60.20
$\Delta q(e^-)$	+0.10	+0.12	+0.10	+0.10

[a] Distances are in Å, angles in deg (for the $r_{(HC)}$ bond length the average value is reported). The calculations with the Gaussian basis sets 6-311++G(d,p) are labeled with G.

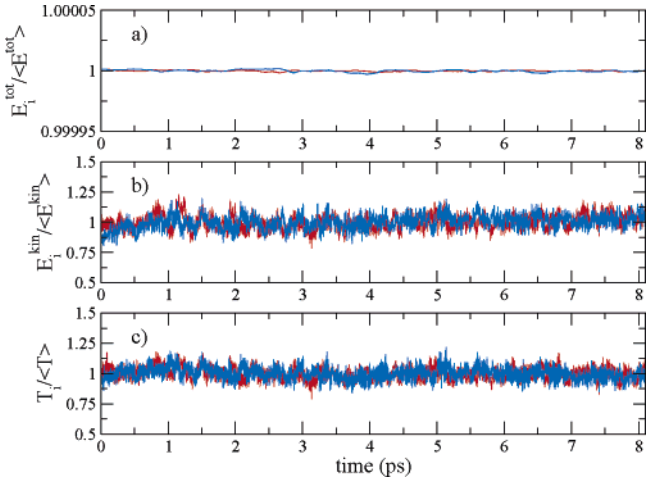

Figure 1. Variation of the total energy (a), of the fictitious electronic kinetic energy (b), and of the temperature (c). Blue and red lines refer to the Li^+ and Cl^- ions, respectively.

has been adopted to keep the system on the Born−Oppenheimer surface. The choice of these parameters allows a correct energy conservation (oscillation of the instantaneous ratio confined within 10^{-5}) along the simulations run as can be observed from Figure 1. The reduced amount of coupling between electronic and nuclear degrees of freedom is well evident from the absence of a drift in the fictitious kinetic energy of the electrons and in the nuclear temperature of the systems.

After a thermalization at 300 K by velocity scaling, the equation of motions has been integrated with a time step of 5 au (∼0.12 fs) for a total simulation time of ∼8.1 ps in the NVE ensemble, storing the atomic coordinates and velocities every 5 steps for the subsequent analysis. AIM[41] and WFCs[42,43] have been calculated by averaging over 135 configurations for both systems.

3. Results and Discussion

The first insight on the structural reorganization of the solvent molecules around the ions has been obtained from the pair distribution functions, g(**r**). The effects of the different nature of the interactions between the two ions and the methanol

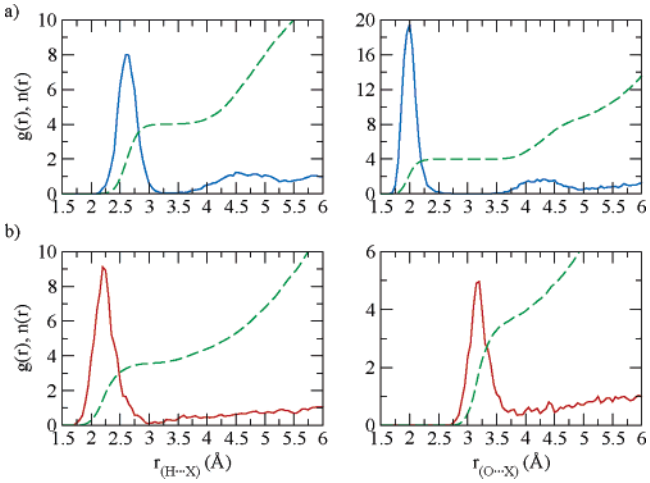

Figure 2. Pair radial distribution functions (full) and running integration number (dotted) for the H···X (left) and O···X contacts: (a) X = Li and (b) X = Cl^-, respectively.

TABLE 2: First Peak Position in the Pair Radial Distribution Functions

	this work	Impey et al.[8] (MD)	Megyes et al.[63] (exp.)
$r_{(O\cdots Li)}$	2.0	1.9	2.06
$r_{(H\cdots Li)}$	2.6	2.9	
$r_{(O\cdots Cl)}$	3.2	3.3	3.16
$r_{(H\cdots Cl)}$	2.2	2.4	

molecules can be observed in Figure 2, where the g(**r**) functions related to the O···X and H···X distance, with X = Li^+ and Cl^-, are reported.

The two ions have nearest neighbor atoms of different species: the lithium cation interacts primarily with the oxygens and the chloride anion with the hydrogens of the solvent molecules. The coordination number, directly obtained from the integration of the first peak of g(**r**), is 4.00 for the cation and 3.56 for the anion. The first peak position in the g(**r**) is in excellent agreement with experiments[63] as can be seen from Table 2, where a comparison with previous classical MD[8] simulations is also reported.

The ab initio H···Cl distance is shorter than that obtained by classical molecular dynamics simulations. It is not possible to explain this difference on the basis of electrostatic interactions, since the charges obtained by AIM are very close to those adopted in the classical simulations.[8] However, it should be considered that these latter do not take into account polarization or charge-transfer effects that, as will be shown, are relevant for these systems.

Despite the excellent agreement in the first peak position in g(**r**), the coordination number differs from the experimental one. In fact, from X-ray measurements[63] a hexacoordination environment for the cation has been proposed. However, it should be mentioned that a precise localization of the lithium ion by X-rays is not possible due to the low elastic scattering coefficient of this species. On the other hand, previous classical[8] and the present ab initio molecular dynamics simulation both predict a coordination number of 4, as displayed for a typical configuration in Figure 3, and by the structural parameters reported in Figure 4. The same value has been obtained for Li^+ in water by classical,[14,15,64−66] QM/MM,[67,68] and ab initio simulations,[28,69] while both the tetrahedral and octahedral coordination have been suggested from experiments.[1] Since the methanol molecular volume is larger than that of water[28] and the source of the interaction is essentially the same (as confirmed also by the

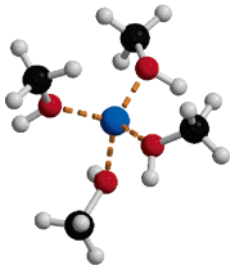

Figure 3. Snapshot of the first solvation shell of the lithium cation.

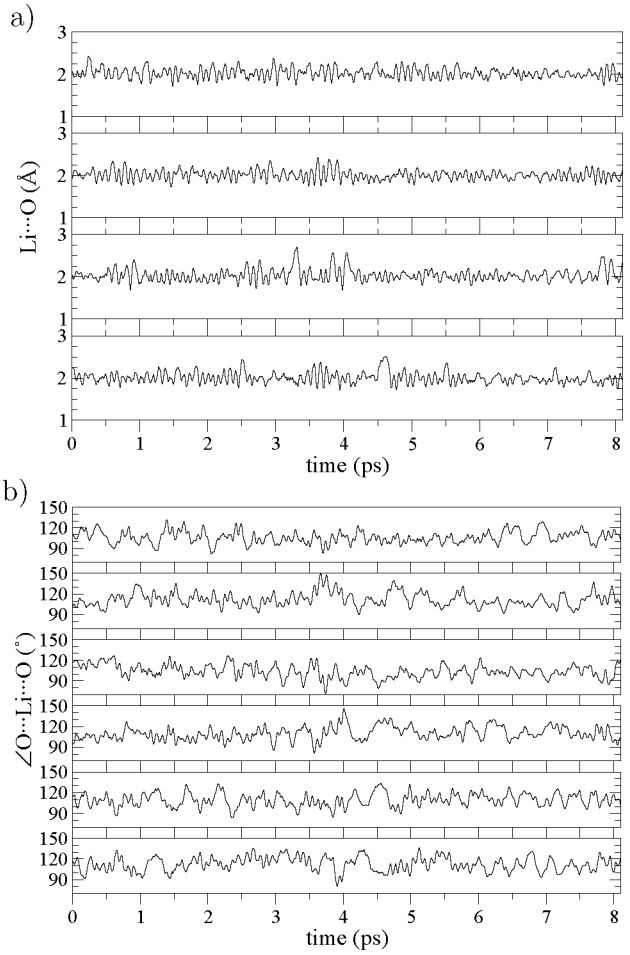

Figure 4. (a) Li···O distances (in Å) along the simulation run. (b) O···Li···O angle (in deg) along the simulation run. Both distances and angles refer to solvent molecule in the first coordination shell.

first peak position in the g(**r**), at 1.96 Å) it would be difficult to explain a coordination number of 6 as proposed on the basis of X-ray scattering experiments.[63] The coordination number of 4 for Li^+ has also been suggested by recent Electron Spray Ionization (ESI) experiment, followed by infrared measurements.[70]

The structural reorganization of the solvation shell around the chloride ion is more complex and the number of molecules involved in the cage is not as well defined as for the cation. In fact, the coordination number obtained from experiments or from simulations ranges from 4 to 6. In particular, in previous classical molecular dynamics simulations[8,71] the coordination number of the chloride has been observed to be 5 by Impey et al.[8] and 6.3 by Sesé et al.[71] The latter point out that "in the case of Cl^- MD results do not reproduce the experimental values", referring to an experimental value of 3 ± 1 for the number of solvent molecules in the first solvation shell and ascribing this discrepancy to the nonpolarizable model used in their calulations. In the present work the chloride ion coordinates essentially 3 or 4 solvent molecules in good agreement with the experimental value quoted by Sesé et al.,[71] but other clusters are also observed, as can be seen from Figure 5. A series of first solvation shells with different chloride coordination number extracted from the simulation is shown in Figure 6.

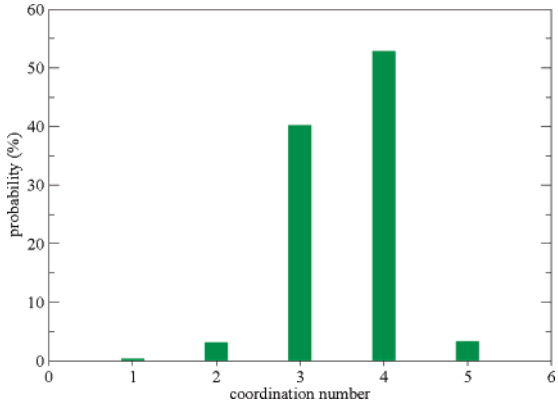

Figure 5. Probability distribution of the coordination number for the chloride anion.

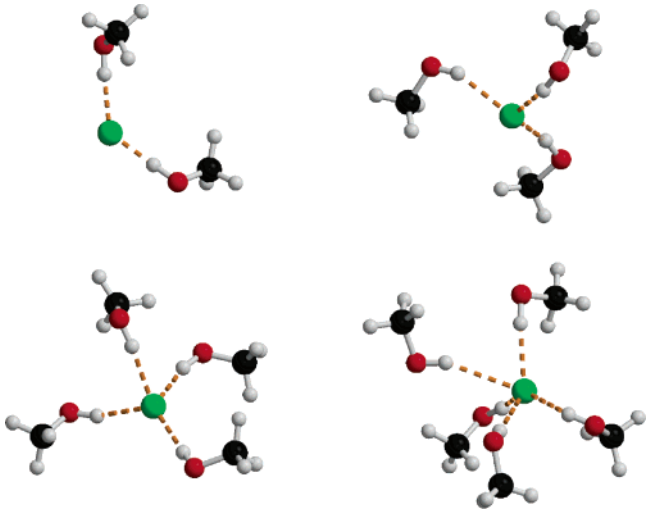

Figure 6. First solvation shell of the chloride with increasing coordination number. The H bonds are shown with an orange dashed line.

The present results are supported by the more recent experimental findings[72−75] and by previous CPMD simulations on HCl[31,32] or Cl^- [51] in water. In fact, the coordination shell of the chloride in water is made of up to five solvent molecules, but a definition of the coordination number is strongly dependent on the geometrical criteria adopted to decide if a molecule is considered bonded or not to the ion. In the simulation of Heuft et al.,[51] for example, the coordination number ranges from a value close to five to one close to six simply by changing the reference distance from Cl···H to Cl···O. To establish the coordination number of the bromide ion in water and to overcome this problem, Raugei and Klein[34,35] have adopted the geometrical criteria usually chosen to characterize the hydrogen bond.[64] In the present work, we have followed the same procedure, with threshold values of $r_{(H\cdots Cl)} < 3.0$ Å, $r_{(O\cdots Cl)} < 3.9$ Å, and $\theta_{(HO\cdots Cl)} < 40°$.

The experimental coordination number of the chloride ion has been obtained from INS[75] and EXAFS[74] meausurements and found to be 3.6(5) for a solution of LiCl 5.8 M and 3.4 ± 0.3 for a 1 M solution of Cl^-. Values of 4 have been obtained

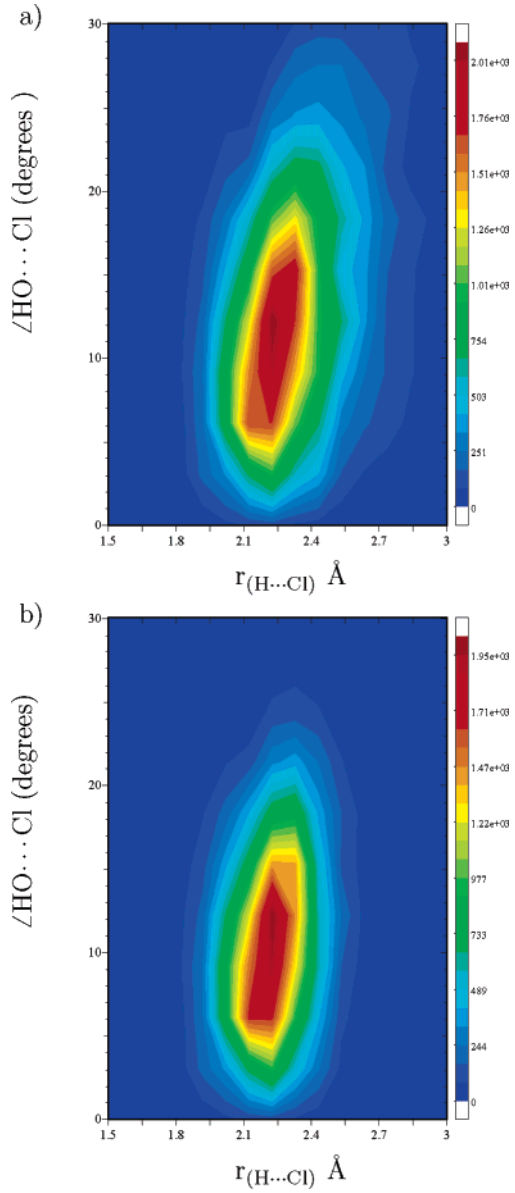

Figure 7. g(**r**,θ) weighted functions for the HO···Cl interactions obtained with the classical (a) and with the new (b) definition of the H bond.[52,76]

by mass spectrometry[72] and by infrared vibrational spectroscopy,[73] as values appropriate for the best description of the experimental findings. These values are very close to 3.57 computed in the present work.

To characterize the configuratonal space between the chloride ion and the methanol molecules the weighted g(**r**,θ) functions of the hydrogen bond have been computed both with the classical geometrical criteria and with the more appropriate function, introduced in a previous work[52] in the study of the H-bond dynamics in liquid methanol. In Figure 7 the two functions are compared and appear to be quite similar.

Even if the intermolecular H···Cl distance is larger than the O···H distance in liquid methanol, the hydrogen bond is stronger for the solvated Cl^- ion. The binding energy is in fact -63.81 kJ mol^{-1} for the Cl···H interaction and -19.77 kJ mol^{-1} for O···H at the BLYP/6-311++G(d,p) level of theory.[77,78] This can be explained on the basis of both the electrostatic interactions and the charge transfer. To evaluate the charge transfer between Cl^- and the solvent molecules, a population analysis with the AIM[41] method has been performed, adopting the

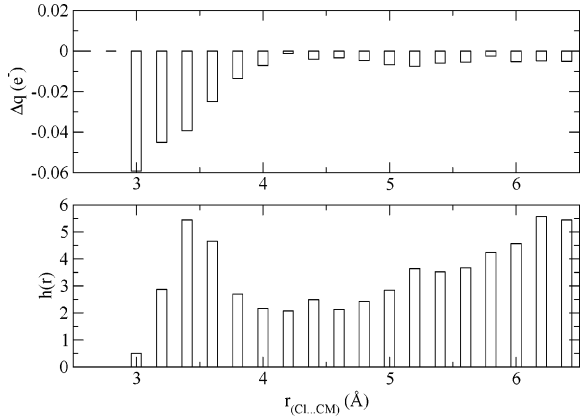

Figure 8. $\Delta q(e^-)$ (top panel) and h(**r**) (bottom panel) as a function of the $r_{(CL\cdots CM)}$.

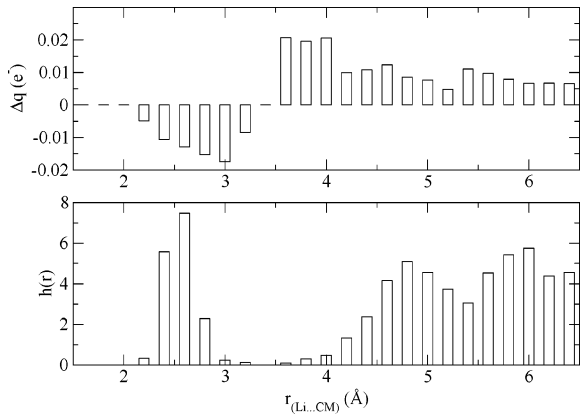

Figure 9. $\Delta q(e^-)$ (top panel) and h(**r**) (bottom panel) as a function of the $r_{(Li\cdots CM)}$.

algorithm of Uberuaga et al.[79] The charge transferred amount, $\Delta q(e^-)$, as a function of the $r_{(Cl...CM)}$ (where CM indicates the methanol center of mass) has been reported in Figure 8 along with the corresponding pair distribution function, h(**r**), between the Cl^- and the methanol center of mass.

The H-bond interaction involves a charge transfer from the Cl^- ion toward the solvent molecules. Therefore, the nearest neighbor molecules of the chloride become negatively charged. The presence of a net negative charge localized in the first coordination shell produces a lower stability of the cage than for the cation.

This behavior can be further explained by comparing with the charge transferred amount, $\Delta q(e^-)$, between the cation and the solvent molecules. As can be observed from Figure 9, the sign of the solvent molecules of the first shell is opposite to both that of the cation and that of the molecules in the second shell.

In fact, the central positive ion attracts charge from the first solvation shell molecules, becoming less positively charged ($+0.8e^-$). On the other side, an amount of charge is transferred from the second to the first solvation shell through the H-bond network. The net balance will then produce a negatively charged first solvation shell and a positively charged second shell. This charge distribution determines a more tight solvent reorganization than in the pure liquid, as confirmed by the shift of the second shell peak from 4.75 to 4.65 Å. A similar behavior has been observed also for Li^+ [14,15] in water and to a major extent for ions with a larger charge.[15]

The H-bond interactions and the charge transfer between the chloride and the neighboring molecules of methanol give raise

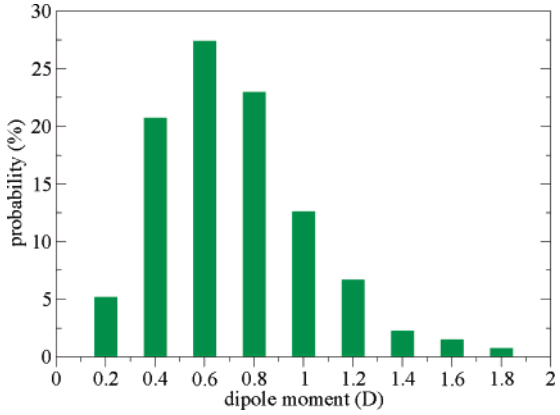

Figure 10. Induced dipole moment distribution of the chloride anion.

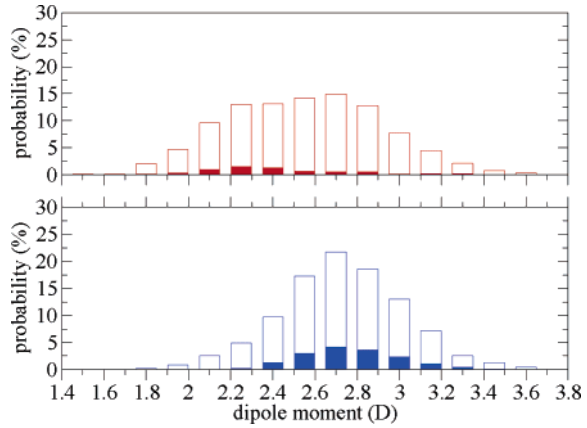

Figure 11. Dipole moment distribution for Cl^- (top panel) and Li^+ (bottom panel): the colored bar refers to the dipole moment distribution of the first solvation shell molecules.

to an induced polarization of the ion, which can be monitored by computing the induced dipole moment. The distribution of the dipole moment is shown in Figure 10 and ranges up to 1.8 D. This distribution is very close to that obtained in a CPMD simulation of $AlCl_3$ in water,[21] using the HCTH exchange and correlation function.[80]

The distribution obtained in the present work is also in agreement with CPMD simulations in water of the Br^- ion reported by Raugei and Klein[34,35] and is only at variance with the values of 4 or 5 D found by Heuft and Meijer[51] with a molecular dynamics simulation of Cl^- in water with an approach completely analogous to ours. The difference in this case can be due to the different sampling used since Heuft and Meijer[51] report the result of an average over only 6 configurations compared to the 135 configurations used in the present work. As a whole a dipole moment in the range of 4−5 D appears quite unreasonable impling an electron at a 4−5 Å distance.

The behavior of the dipole moment of the solvent molecules in the presence of the two different ions is displayed in Figure 11, where the distribution of the average dipole moment is compared with the dipole moment of the first shell molecules. It can be seen that the dipole moment of the first shell in the case of Li^+ reproduces closely the dipole distribution in all the solvents. In fact the dipole moment of the first shell (2.76 D) is only slightly larger than the average of 2.73 D and should be compared with the average value of 2.64 D in the pure solvent. On the contrary, in the Cl^- solution the first shell molecules have a significantly lower value (2.44 D) than the average (2.55 D).

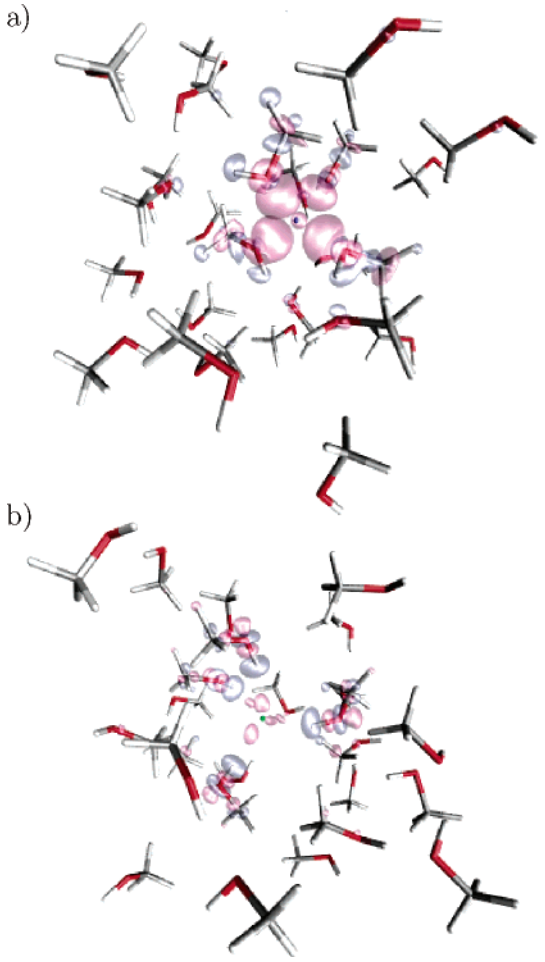

Figure 12. Density difference isosurfaces, $\Delta\rho$ at $\pm$ 0.003 (au): (a) Li^+ solution and (b) Cl^- solution. Volumes with negative values are shown in mauve, volumes with positive values are in iceblue.

As described above, the interactions between ions and solvent involve many terms: charge transfer, polarization effects, H-bonds, etc. These mutual perturbations reflect on the electronic structure either of the ions or of the solvent as can be observed in Figure 12, where the differences between the electron densities, $\Delta\rho$ of the two systems, are reported:

$$\Delta\rho = \rho_{\text{ion+solvent}} - (\rho_{\text{ion}} + \rho_{\text{solvent}}) \qquad (1)$$

It is possible to note from both figures that the electronic density perturbations are essentially localized in the region of the first solvation shell, whereas the outer molecular electronic densities are only slightly affected by the presence of the ion.

The different structural arrangements of the solvent cage around the Li^+ and Cl^- ions show their effects also in the vibrational spectra calculated as the power spectra of the velocity autocorrelation function (PSVACF) and shown in Figure 13. The nuclear motion has been treated classically and therefore zero point energy is not included in the calculation. In principle this implies that in the high-frequency region the nuclear motion explores a more harmonic potential well. We have not attempted to correct the classical time correlation functions to take the zero point energy into account. In a recent paper Ramírez et al.[81] have carried out a path integral molecular dynamics calculation of water cluster with H^+ that takes zero point energy into account explicitely. They show that the zero point energy is quite important where the system has a double minimum structure with a barrier height that allows for the quantum

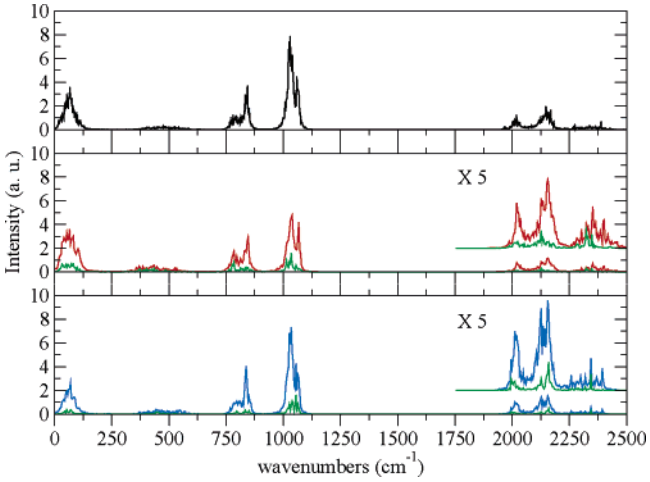

Figure 13. PSVACF for the liquid methanol (top panel), the Cl^- system (central panel), and the Li^+ system (bottom panel). The green lines refer to the PSVACF of the first solvation shell molecules. The intensity of the PSVACF in the region between 1750 and 2500 cm^{-1} for the Li^+ and Cl^- solutions is enhanced by a factor of 5 for a better visualization of the spectral features.

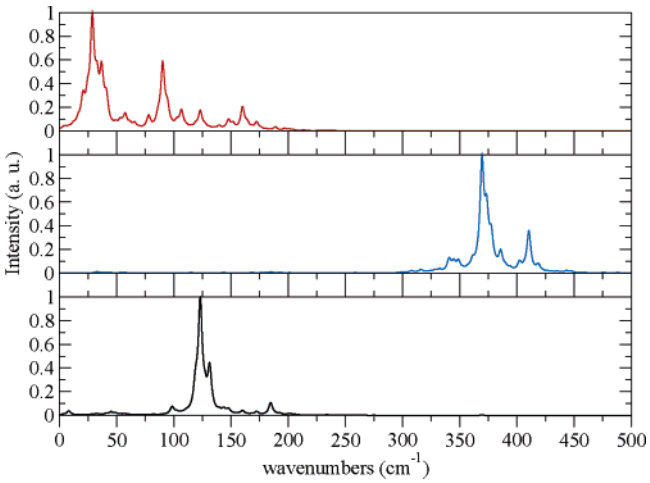

Figure 14. PSVACF of the chloride (top panel) and lithium (central panel) ions and of the cage of the solvent molecules in the Li^+ system.

tunneling. This is not the case for the systems studied in the present work. In these more general cases the effect of zero point energy inclusion is mainly to broaden the vibrational spectrum (in the ν_{O-D} region) and to produce a small frequency shift. It is evident from these findings that the results on the vibrational density of states will not be greatly affected by the neglect of zero point energy.

The OD stretching region is particularly noteworthy. Compared to pure methanol a red shift is observed as a consequence of the hydrogen bond formation. This is particularly evident considering the contribution in this spectral region of the molecules of the first solvation shell. Such a red shift is not observed in the Li^+ solution.

The power spectra of the velocity autocorrelation function of the two solvated ions have also been calculated and are shown in Figure 14. The hydrogen bonded Cl^- ion exhibits a number of bands in the range from 35 to approximatively 160 cm^{-1}, as observed also from classical molecular dynamics simulation,[71] while the Li^+ ion shows bands between 350 and 420 cm^{-1}. This increase in frequency is explained in part by the different masses of the ions and in part by the strenght of the electrostatic interaction of the Li^+ ion with the cage compared to the hydrogen bond of Cl^-.[71,82] Since the solvent cage around the Li^+ ion is characterized by a well-defined structure it is possible to extract a number of frequencies associated with the modulation of the inertia moment of the first shell molecules. In particular it is found (see Figure 14, lower panel) that the breathing mode of the cage occurs at ~132 cm^{-1}, a frequency very close to that obtained for a $Li^+ + 4CH_3OH$ cluster[78,83] at the BLYP/6-31++G(d,p) level of theory.

4. Conclusions

In the present work several details have been obtained on the structure and dynamics of the solvation of Li^+ and Cl^- in liquid methanol from ab initio CPMD simulations.

The coordination number of the lithium cation and of the chloride anion has been computed and compared with the most recent experimental measurements,[63,70−75] showing that the first is tetracoordinated as in water, whereas for the latter the coordination number (3.56) is lower than in water. In particular, the first solvation shell of both ions has been characterized giving a detailed picture of the solvent reorganization and explaining the origin of the higher stability of the Li^+ cage. The charge transfer between the solvent molecules and the ions and the polarization effects have been analyzed in term of AIM and WFCs, showing that the first solvation shell of Li^+ is negatively charged whereas the second solvation shell is positively charged. This type of interaction plays a key role in the stability of the cage and this is also confirmed by structural and spectroscopic analysis. In contrast with the well-defined solvation structure of Li^+, the H-bond interactions with the chloride ion produce a more loosely defined solvation shell, characterized by a quite large induced dipole moment on the ion.

Acknowledgment. The authors would like to thank Prof. M. L. Klein and Dr. S. Raugei for helpful discussions. This work was supported by the Ministero dell'Istruzione, dell'Università e della Ricerca (MIUR), and by the European Union (contract nos. ERB-FMGE-CT950017 and HRPI-CT1999-00111).

References and Notes

(1) Ohtaki, H.; Radnai, T. *Chem. Rev.* **1993**, *93*, 1157−1204.
(2) Doyle, D. A.; Cabral, J. M.; Pfuetzner, R. A.; Kuo, A.; Gulbis, J. M.; Cohen, S. L.; Chait, B. T.; MacKinnon, R. *Science* **1998**, *280*, 69−77.
(3) Zhou, Y.; Morais-Cabral, J. H.; Kaufman, A.; MacKinnon, R. *Nature* **2001**, *414*, 43−48.
(4) Roux, B. *Curr. Opin. Struct. Biol.* **2002**, *12*, 182−189.
(5) Giorgetti, A.; Carloni, P. *Curr. Opin. Chem.* **2001**, *414*, 43−48.
(6) Sprik, M.; Impey, R. W.; Klein, M. L. *Phys. Rev. Lett.* **1986**, *56*, 2326−2329.
(7) Martyna, G. J.; Klein, M. L. *J. Chem. Phys.* **1992**, *96*, 7662−7671.
(8) Impey, R. W.; Sprik, M.; Klein, M. L. *J. Am. Chem. Soc.* **1987**, *109*, 5900−5904.
(9) Jorgensen, W. L.; Bigot, B.; Chandrasekhar, J. *J. Am. Chem. Soc.* **1982**, *104*, 4584−4591.
(10) Chandrasekhar, J.; Jorgensen, W. L. *J. Chem. Phys.* **1982**, *77*, 5080−5089.
(11) Sesé, G.; Padró, J. A. *J. Chem. Phys.* **1998**, *108*, 6347−6352.
(12) Islam, M. S.; Pethrick, R. A.; Pugh, D. *J. Phys. Chem. A* **1998**, *102*, 2201−2208.
(13) Masella, M.; Cuniasse, P. *J. Chem. Phys.* **2003**, *113*, 1866−1873.
(14) Spångberg, D.; Hermansson, K. *Chem. Phys.* **2004**, *300*, 165−176.
(15) Spångberg, D. Cation Solvation in Water and Acetonitrile from Theoretical Calculations. Ph.D. Thesis, Uppsala, 2003.
(16) Hutter, J.; Alavi, A.; Deutch, T.; Bernasconi, M.; Goedecker, S.; Marx, D.; Tuckerman, M.; Parrinello, M. *CPMD*; MPI für Festkörperforschung and IBM Zurich Research Laboratory: Stuttgart, Germany, 1995−1999.
(17) Car, R.; Parrinello, M. *Phys. Rev. Lett.* **1985**, *55*, 2471−2474.
(18) Tse, J. S. *Annu. Rev. Phys. Chem.* **2002**, *53*, 249−290.
(19) White, J. A.; Schwegler, E.; Galli, G.; Gygi, F. *J. Chem. Phys.* **2000**, *113* (11), 4668−4673.

(20) Bakó, I.; Hutter, J.; Pálinkás, G. *J. Chem. Phys.* **2002**, *117*, 9838−9843.
(21) Ikeda, T.; Hirata, M.; Kimura, T. *J. Chem. Phys.* **2003**, *119* (23), 12386−12392.
(22) Ramaniah, L. M.; Bernasconi, M.; Parrinello, M. *J. Chem. Phys.* **1999**, *111* (4), 1587−1591.
(23) Lightstone, F. C.; Schwegler, E.; Hood, R. Q.; Gygi, F.; Galli, G. *Chem. Phys. Lett.* **2001**, *343*, 549−555.
(24) Marx, D.; Sprik, M.; Parrinello, M. *Chem. Phys. Lett.* **1997**, *273*, 360−366.
(25) Naor, M. M.; Nostrand: K. V.; Dellago, C. *Chem. Phys. Lett.* **2003**, *369*, 159−164.
(26) Blumbergerer, J.; Sprik, M. *J. Phys. Chem. B* **2004**, *108*, 6529−6535.
(27) Blumberger, J.; Bernasconi, L.; Tavernelli, I.; Vuilleumier, R.; Sprik, M. *J. Am. Chem. Soc.* **2004**, *126*, 3928−3938.
(28) Lyubartsev, A. P.; Laasonen, K.; Laaksonen, A. *J. Chem. Phys.* **2001**, *114* (7), 3120−3126.
(29) Vuilleumier, R.; Sprik, M. *J. Chem. Phys.* **115**, *8*, 3454−3468.
(30) Tuckerman, M.; Laasonen, K.; Sprik, M.; Parrinello, M. *J. Chem. Phys.* **1995**, *103*, 150−161.
(31) Laasonen, K.; Klein, M. L. *J. Am. Chem. Soc.* **1994**, *116*, 11620−11621.
(32) Laasonen, K. E.; Klein, M. L. *J. Phys. Chem. A* **1997**, *101*, 98−102.
(33) Dal Peraro, M.; Raugei, S.; Carloni, P.; Klein, M. L. *Chem. Phys. Chem.* in press.
(34) Raugei, S.; Klein, M. L. *J. Am. Chem. Soc.* **2001**, *123*, 9484−9485.
(35) Raugei, S.; Klein, M. L. *J. Chem. Phys.* **2002**, *116*, 196−202.
(36) Delle Site, L.; Alavi, A.; Lynden-Bell, R. M. *Mol. Phys.* **1999**, *96* (11), 1683−1693.
(37) Delle Site, L.; Alavi, A.; Lynden-Bell, R. M. *J. Mol. Liq.* **2002**, *98*−*99*, 79−86.
(38) Nadig, G.; Zant, L. C. V.; Dixon, S. L.; Merz, K. M., Jr. *J. Am. Chem. Soc.* **1998**, *120*, 5593−5594.
(39) van der Vaart, A.; Merz, K. M., Jr. *J. Am. Chem. Soc.* **1999**, *121*, 9182−9190.
(40) Gogonea, V.; Suárez, D.; van der Vaart, A.; Merz, K. M., Jr. *Curr. Opin. Struct. Biol.* **2001**, *11*, 217−223.
(41) Bader, R. F. W. *Chem. Rev.* **1991**, *91*, 893−928.
(42) Marzari, N.; Vanderbilt, D. *Phys. Rev. B* **1997**, *56*, 12847−12862.
(43) Silvestrelli, P. L.; Marzari, N.; Vanderbilt, D.; Parrinello, M. *Solid State Commun.* **1998**, *107* (1), 7−11.
(44) Koritsanszky, T. S.; Coppens, P. *Chem. Rev.* **2001**, *101*, 1583−1627.
(45) Flaig, R.; Koritsanszky, T.; Dittrich, B.; Wagner, A.; Luger, P. *J. Am. Chem. Soc.* **2002**, *124*, 3407−3417.
(46) Szefczyk, B.; Sokalski, W. A.; Leszczynski, J. *J. Chem. Phys.* **2002**, *117* (15), 6952−6958.
(47) Gálvez, O.; Gómez, P. C.; Pacios, L. F. *J. Chem. Phys.* **2001**, *115* (24), 11166−11184.
(48) Gálvez, O.; Gómez, P. C.; Pacios, L. F. *J. Chem. Phys.* **2003**, *118* (11), 4878−4895.
(49) Pagliai, M.; Raugei, S.; Cardini, G.; Schettino, V. *Phys. Chem. Chem. Phys.* **2001**, *3*, 2559−2566.
(50) Pagliai, M.; Raugei, S.; Cardini, G.; Schettino, V. *Phys. Chem. Chem. Phys.* **2001**, *3*, 4870−4873.
(51) Heuft, J. M.; Meijer, E. J. *J. Chem. Phys.* **2003**, *119*, 11788−11791.
(52) Pagliai, M.; Cardini, G.; Righini, R.; Schettino, V. *J. Chem. Phys.* **2003**, *119* (13), 6655−6662.
(53) Handgraaf, J.-W.; van Erp, T. S.; Meijer, E. J. *Chem. Phys. Lett.* **2003**, *367*, 617−624.
(54) Boero, M.; Terakura, K.; Ikeshoji, T.; Liew, C. C.; Parrinello, M. *Phys. Rev. Lett.* **2000**, *85* (15), 3245−3248.
(55) Boero, M.; Terakura, K.; Ikeshoji, T.; Liew, C. C.; Parrinello, M. *J. Chem. Phys.* **2001**, *115* (5), 2219−2227.
(56) Silvestrelli, P. L.; Parrinello, M. *Phys. Rev. Lett.* **1999**, *82* (16), 3308−3311.
(57) Silvestrelli, P. L.; Parrinello, M. *J. Chem. Phys.* **1999**, *111* (8), 3572−3580.
(58) Troullier, N.; Martins, J. L. *Phys. Rev. B* **1991**, *43*, 1993−2006.
(59) Kleinman, L.; Bylander, D. M. *Phys. Rev. Lett.* **1982**, *48*, 1425−1428.
(60) Goedecker, S.; Teter, M.; Hutter, J. *Phys. Rev. B* **1996**, *54* (3), 1703−1710.
(61) Becke, A. D. *Phys. Rev. A* **1988**, *38* (6), 3098−3100.
(62) Lee, C.; Yang, W.; Parr, R. G. *Phys. Rev. B* **1988**, *37* (2), 785−789.
(63) Megyes, T.; Radnai, T.; Grósz, T.; Pálinkàs, G. *J. Mol. Liq.* **2002**, *101* (1−3), 3−18.
(64) Impey, R. W.; Madden, P. A.; McDonald, I. R. *J. Phys. Chem.* **1983**, *87*, 5071−5083.
(65) Egorov, A. V.; Komolkin, A. V.; Chizhik, V. I.; Yushmanov, P. V.; Lyubartsev, A. P.; Laaksonen, A. *J. Phys. Chem. B* **2003**, *107*, 3234−3242.
(66) Lee, S. H.; Rasaiah, J. C. *J. Phys. Chem.* **1996**, *100*, 1420−1425.
(67) Loeffler, H. H.; Rode, B. M. *J. Chem. Phys.* **2002**, *117* (1), 110−117.
(68) Öhrn, A.; Karlström, G. *J. Phys. Chem. B* **2004**, *108*, 8452−8459.
(69) Rempe, S. B.; Pratt, L. R.; Hummer, G.; Kress, J. D.; Martin, R. L.; Redondo, A. *J. Am. Chem. Soc.* **2000**, *122*, 966−967.
(70) Wu, C.-C.; Wang, Y.-S.; Chandhuri, C.; Jiang, J. C.; Chang, H.-C. *Chem. Phys. Lett.* **2004**, *388*, 457−462.
(71) Sesé, G.; Guáurdia, E.; Padró, J. A. *J. Chem. Phys.* **1996**, *105* (19), 8826−8834.
(72) Megyes, T.; Radnai, T.; Wakisaka, A. *J. Phys. Chem. A* **2002**, *106*, 8059−8065.
(73) Cabarcos, O. M.; Weinheimer, C. J.; Martínez, T. J.; Lisy, J. M. *J. Chem. Phys.* **1999**, *110*, 9516−9526.
(74) Ozutsumi, K.; Ohtaki, H. *Pure Appl. Chem.* **2004**, *76*, 91−96.
(75) Adya, A. K.; Kalugin, O. N. *J. Chem. Phys.* **2000**, *113*, 4740−4750.
(76) Pagliai, M.; Raugei, S.; Cardini, G.; Schettino, V. *J. Mol. Struct. THEOCHEM* **2003**, *630* (1−3), 141−149.
(77) Structure minimization and binding energies with BSSE correction for the $Cl^- + CH_3OH$ and methanol dimer have been performed at the BLYP/6-311++G(d,p) level of theory with the Gaussian 98 rev. A11 suite of programs.[78]
(78) Frisch, M. J.; Trucks, G. W.; Schlegel, H. B.; Scuseria, G. E.; Robb, M. A.; Cheeseman, J. R.; Zakrzewski, V. G.; Montgomery, J. A., Jr.; Stratmann, R. E.; Burant, J. C.; Dapprich, S.; Millam, J. M.; Daniels, A. D.; Kudin, K. N.; Strain, M. C.; Farkas, O.; Tomasi, J.; Barone, V.; Cossi, M.; Cammi, R.; Mennucci, B.; Pomelli, C.; Adamo, C.; Clifford, S.; Ochterski, J.; Petersson, G. A.; Ayala, P. Y.; Cui, Q.; Morokuma, K.; Malick, D. K.; Rabuck, A. D.; Raghavachari, K.; Foresman, J. B.; Cioslowski, J.; Ortiz, J. V.; Stefanov, B. B.; Liu, G.; Liashenko, A.; Piskorz, P.; Komaromi, I.; Gomperts, R.; Martin, R. L.; Fox, D. J.; Keith, T.; Al-Laham, M. A.; Peng, C. Y.; Nanayakkara, A.; Gonzalez, C.; Challacombe, M.; Gill, P. M. W.; Johnson, B.; Chen, W.; Wong, M. W.; Andres, J. L.; Gonzalez, C.; Head-Gordon, M.; Replogle, E. S.; Pople, J. A. *Gaussian 98*, Revision A.11; Gaussian Inc.: Pittsburgh, PA, 1998.
(79) Uberuaga, B. P.; Batista, E. R.; Jónsson, H. *J. Chem. Phys.* **1999**, *111*, 10664−10669.
(80) Hamprecht, F. A.; Cohen, A. J.; Tozer, D. J.; Handy, N. C. *J. Chem. Phys.* **1998**, *109*, 6264−6271.
(81) Ramírez, R.; López-Ciudad, T.; Kumar P, P.; Marx, D. *J. Chem. Phys.* **2004**, *121* (9), 3973−3983.
(82) Guillot, B.; Marteau, P.; Obriot, J. *J. Chem. Phys.* **1990**, *93* (9), 6148−6164.
(83) Structure minimization and normal frequencies calculation for the $Li^+ + 4CH_3OH$ cluster in the S_4 point group symmetry have been performed at the BLYP/6-311++G(d,p) level of theory with the Gaussian 98 rev. A11 suite of programs.[78]